JACS
JOURNAL OF THE AMERICAN CHEMICAL SOCIETY
Article
pubs.acs.org/JACS

Enhanced Brightness Emission-Tuned Nanoparticles from Heterodifunctional Polyfluorene Building Blocks

Christoph S. Fischer, Moritz C. Baier, and Stefan Mecking*

Chair of Chemical Materials Science, Department of Chemistry, University of Konstanz, 78464 Konstanz, Germany

Supporting Information

ABSTRACT: Three-coordinate complexes (bromo)[4-(2,2-dimethyl-1,3-dioxolan-4-yl)-phenyl](tri-*tert*-butyl-phosphine) palladium (**1**) and (bromo){4-[(tetrahydro-2*H*-pyran-2-yloxy)methyl]phenyl}(tri-*tert*-butyl-phosphine)palladium (**2**) were used to initiate Suzuki–Miyaura chain growth polymerization of 7′-bromo-9′,9′-dioctyl-fluoren-2′-yl-4,4,5,5-tetramethyl-[1,3,2]dioxaborolane (**3**). The polymerization was optionally terminated by end-capping with red-emitting *N*-(2-ethylhexyl)-1,6-bis(4-*tert*-octylphenoxy)-9-(4,4,5,5-tetramethyl-[1,3,2]dioxaborolan-2-yl)-perylene-3,4-dicarboximide. Heterodisubstituted polyfluorenes of adjustable molecular weights between 5×10^3 and 1.0×10^4 g mol^{-1} and narrow molecular weight distribution ($M_w/M_n < 1.2$), bearing precisely one or two hydroxyl groups on one chain end and optionally a dye-label on the opposite end, were obtained virtually devoid of any side-products. Covalent attachment of polyethylene glycol ($M_n = 2 \times 10^3$ g mol^{-1}) to the reactive end groups yielded amphiphilic block copolymer, which afforded stable nanoparticles with diameters in the range of 25–50 nm when dispersed in water. These particles exhibited a bright fluorescence emission with quantum yields as high as $\Phi = 84\%$, which could optionally be tuned to longer wavelengths by energy transfer to the perylene monoimide dye. The heterodifunctional nature of these polyfluorenes is crucial for a bright and enduring fluorescence brightness as revealed by comparison to nanoparticles containing physically mixed dye. Further addition of terrylene diimide dye to the nanoparticles of perylene-end-capped polyfluorene block copolymers allows for an energy cascade resulting in emission exclusively in the deep red and near-infrared regime.

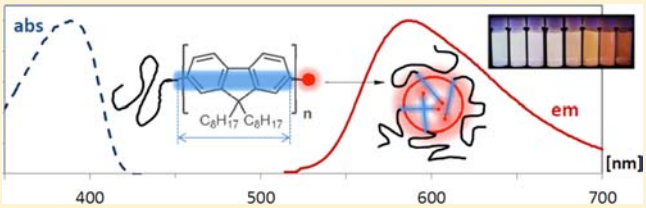

INTRODUCTION

Luminescent nanoparticles are of strong interest related to their applications in optoelectronics,[1,2] live cell imaging,[3−5] and biosensing. Among the different classes of materials studied,[6−9] conjugated polymer nanoparticles[10] favorably combine high absorption coefficients, fluorescence quantum yields, and extraordinarily high nonlinear optical absorption cross sections.[9d,11] By comparison to inorganic quantum dots, the absence of toxic metals can be advantageous in terms of toxicity.[9a,e] Most frequently, studies of such luminescent particles have employed polyfluorene as the conjugated polymer.[1,12] Commonly, these nanoparticles employ physisorbed surfactants as the stabilizing agent necessary to provide colloidal stability and prevent aggregation. This can be problematic in fundamental studies as well as applications of such nanoparticles as possible desorption of surfactant adds an unknown parameter affecting, for example, the particle stability over time or in different environments, such as physiological environments with their variable ion concentration. An elegant alternative approach to nanoparticles in general is their generation from amphiphilic block copolymers. These may form stable core/shell-type particles by self-aggregation in water without the need for further addition of stabilizers.

Block copolymers are synthetically accessible by controlled chain-growth polymerization reactions with sequential addition of various monomers or by linkage of two end-functionalized blocks. However, polyfluorenes are usually prepared by Suzuki–Miyaura polycondensation in a classical step-growth fashion, not amenable to the preparation of block copolymers. The pioneering work of Yokozawa et al. in 2007[13] enabled the synthesis of well-defined polyfluorenes by a controlled chain-growth Suzuki–Miyaura type polymerization reaction of aromatic AB monomers. Chain propagation is initiated by arylpalladium complexes of the general structure [^{t}Bu$_3$P(Br)-Pd–Ar], with the aromatic ligand Ar representing the starting end of the growing polymer chain. As a result of the control over polymerization behavior, the terminal end can be modified by addition of a different boronic ester compound after consumption of the AB type monomer.[14,15] However, the type of chain-end functionality originating from the initiator has been limited to unreactive aromatic hydrocarbon aryls unsuitable for further modifications. The ability of introducing such reactive polymer end groups via the initiator would very much enhance the general scope and power of this synthetic methodology, and provide access to novel narrow distributed polyfluorene materials such as block copolymers.

Here, we report the synthesis of heterodifunctional polyfluorenes by controlled chain-growth Suzuki–Miyaura type polymerization. A chemically reactive functional end

Received: November 23, 2012
Published: December 31, 2012

dx.doi.org/10.1021/ja311497e | *J. Am. Chem. Soc.* 2013, 135, 1148–1154

Scheme 1. Synthetic Approach toward Size-Controlled Diblock Copolymers with End Group Labeling Suitable for Nanoprecipitation[a]

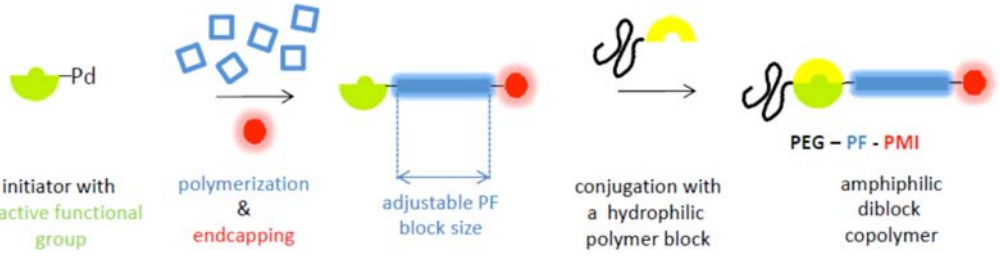

[a]PF = polyfluorene, PEG = polyethylene glycol, PMI = perylene monoimide dye.

group is introduced by a functionalized initiator, and the second chain-end is modified by end-capping with a fluorescent dye, to which an energy transfer can occur. Subsequent conjugation of this polymer chain to a hydrophilic block facilitates the preparation of self-stabilizing emission-tuned conjugated polymer nanoparticles (Scheme 1).

RESULTS AND DISCUSSION

The controlled Suzuki–Miyaura chain-growth polymerization is characterized by incorporation of the aromatic ligand of the Pd initiator at one polymer chain end. To introduce a chain-end functionality into the polymer, tricoordinated Pd complexes with para-substituted phenyl ligands containing reactive functional groups were synthesized and isolated. The functionalization on the aryl moiety consisted of an acetal protected dihydroxy group in case of initiator **1** and a tetrahydropyran (THP) protected hydroxy group for initiator **2** (Scheme 2).

Scheme 2. Synthesis of Initiators 1 and 2 with Protected Functional Groups

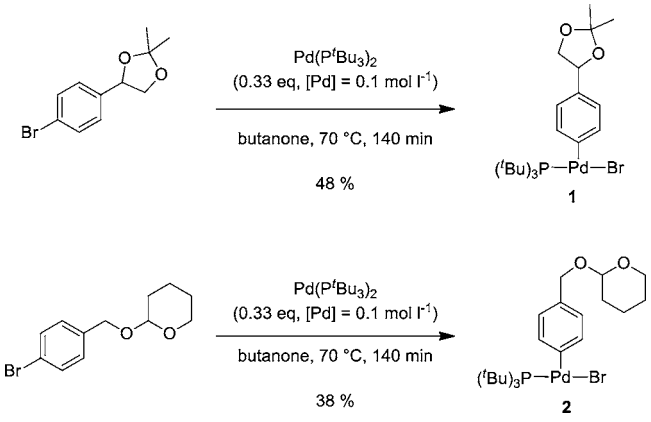

These protecting groups were chosen to remain intact during initiator synthesis and polymerization, however, allowing facile removal under acidic conditions. The key step of the initiator synthesis was the oxidative addition of the phenyl bromide derivatives to the Pd(0) precursor. Because of the formation of side products at elevated reactant conversions, product yields and purities are crucially dependent on the choice of reaction time and temperature. Optimal reaction conditions were found at 70 °C and 140 min reaction time with 3 equiv of aryl halide in butanone as a solvent. Both compounds were isolated in high purity by precipitation from pentane in satisfactory yields of 48% and 38% for complexes **1** and **2**, respectively. Proton NMR spectroscopy corroborates a 1:1 stoichiometry of tri-*t*-butylphosphine to the para-substituted phenyl ligands for both complexes (Figures S1 and S3, Supporting Information). The purity of the compounds is further evidenced by a single ^{31}P NMR resonance. Elemental analyses are in good agreement with theoretical values, and the high-resolution ESI mass spectrum of **1** exhibited signals of Na and K adducts of the desired structure (Figure S2, Supporting Information).

Complexes **1** and **2** smoothly initiated the polymerization of fluorene monomer **3** (Scheme 3) to yield perfectly end-functionalized polymers **PF1** and **PF2**. The remarkably controlled nature of this chain-growth polymerization is reflected by a strictly linear increase in molecular weights versus monomer conversion at a constantly low molecular weight distribution (Figure S11, Supporting Information). As a result, molecular weights can be adjusted by variation of the monomer to initiator ratio (Table 1). Molecular weights ranging from 5×10^3 to about 1.0×10^4 g mol^{-1} corresponding to a degree of polymerization of 10–20 could be obtained with M_w/M_n as low as 1.2. Even higher molecular weights were accessible (e.g., 1.7×10^4 g mol^{-1} by NMR for a monomer to initiator ratio of 40:1), but at the expense of a broader distribution (M_w/M_n = 1.4). MALDI-TOF spectra of **PF1** and **PF2** are characterized by a series of signals, separated by the weight difference of one fluorene repeat unit, corresponding to polymer chains with an initiator-derived end group, with side products being virtually absent (Figure 1). This completely chain-end-functionalized polymer structure allowed the determination of the number average molecular weights by ^{1}H NMR spectroscopy. Within experimental error of the method, theoretically expected and experimentally found degrees of polymerization (calculated from monomer to initiator ratio and degree of conversion) coincided (Table 1). The combined data thus confirm that narrowly distributed polyfluorenes of adjustable molecular weight with one functional end group on every chain were obtained.

End-capping of the chain by a suitable dye (vide infra) was achieved by addition of an excess of a boronic ester compound to the polymerization mixture before quenching the reaction with HCl. A boronic ester-substituted perylene monoimide dye (PMI)[16] was added to the reaction upon almost complete conversion of the fluorene monomer. With a 25-fold excess of this end-capping reagent, the heterodisubstituted structure FG-PF-PMI (Scheme 3, FG: functional group) could be obtained cleanly. The formation of this structure was verified by MALDI-TOF mass spectrometry, which shows exclusively masses of the desired product with only trace amounts at the lower limit of detection of the MALDI-TOF method of nonend-capped polyfluorene present (Figure 2). ^{1}H NMR spectra exhibit

dx.doi.org/10.1021/ja311497e | J. Am. Chem. Soc. 2013, 135, 1148–1154

Scheme 3. Synthesis of End-Functionalized Polyfluorenes PF1, PF2 and PMI End-Capped FG-PF-PMI[a]

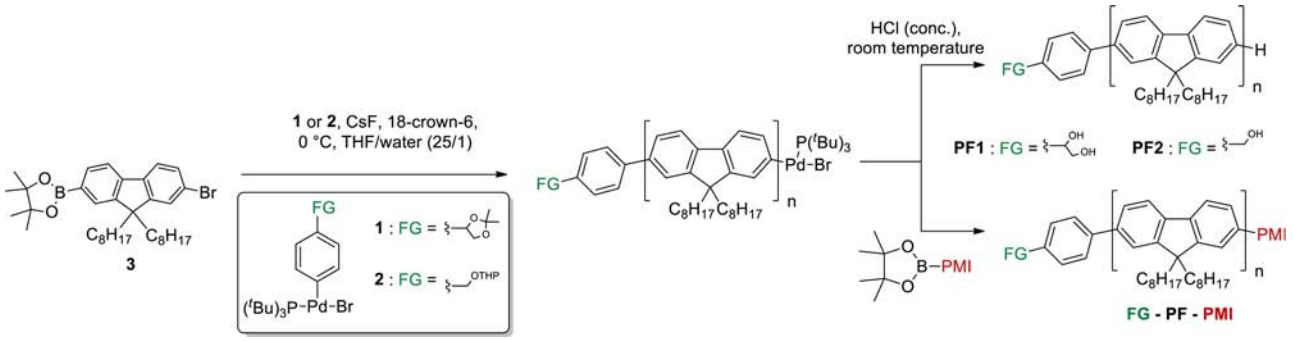

[a]FG = functional group.

Table 1. Polymerization of Fluorene 3 with Initiators 1 and 2[a]

entry	initiator	monomer:initiator	M_n (theo)[b] (g mol^{-1})	M_n (NMR)[c] (g mol^{-1})	M_n (GPC)[d] (g mol^{-1})	M_w/M_n[d]
1	**1**	10:1	3.5×10^3 [e]	4.7×10^3	6.8×10^3	1.15
2	**1**	20:1	6.2×10^3 [f]	8.2×10^3	1.5×10^4	1.25
3	**2**	10:1	3.5×10^3 [e]	4.5×10^3	7.1×10^3	1.20
4	**2**	20:1	6.2×10^3 [f]	6.6×10^3	9.9×10^3	1.19

[a]Reaction conditions: 0 °C; 2−3 h; solvent: THF:H_2O = 25:1; 4 equiv of CsF and 8 equiv of 18-crown-6 with respect to amount of monomer. [b]M_n (theo) = (monomer:initiator ratio) × $M_{repeat\ unit}$ × monomer conversion. [c]Determined by ^{1}H NMR spectroscopy. [d]Determined by GPC in THF at 40 °C versus polystyrene standards. [e]80% monomer conversion. [f]90% monomer conversion (for details, see the Supporting Information).

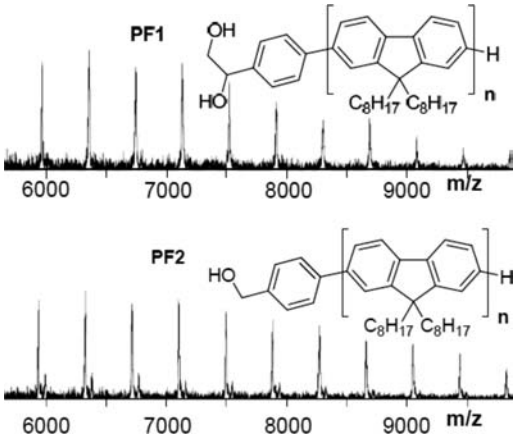

Figure 1. MALDI-TOF mass spectra of **PF1** and **PF2**.

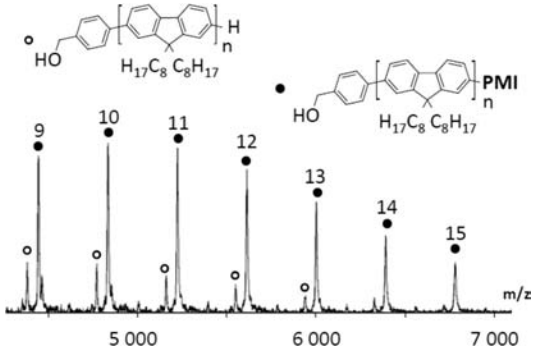

Figure 2. MALDI-TOF mass spectrum of perylene monoimide (PMI)-substituted polyfluorene. Closed and open circles indicate end-capped and non-end-capped chains, respectively. Degrees of polymerization are represented by the numbers above the closed circles.

initiator end and end-capper resonances in a 1:1 ratio (Figure S6, Supporting Information). This confirms that all polyfluorene chains bear exclusively the two desired different end groups within experimental errors (estimated to be ca. 5% or lower). Molecular weight as determined by ^{1}H NMR spectroscopy (M_n = 6.9 × 10^3 g mol^{-1}) was not significantly affected by the introduction of the end-caps, as compared to similar polymerizations without end-capping (cf., Table 1, entries 2 and 4). Likewise, the molecular weight distribution remained low at M_w/M_n = 1.2.

Toward the aim of stable, aqueous nanoparticle dispersions, a hydrophilic segment was attached to the polymer chains to render them amphiphilic (Scheme 1). A hydrophilic polyethylene glycol (PEG) block was covalently linked to the polyfluorene block via amide formation. In a first step, the terminal alcohol of the polyfluorene was converted into a carboxylic acid using succinic anhydride. Subsequently, the polyfluorene acid end group was activated with carbonyldiimidazole (CDI) and reacted with a primary PEG amine (Scheme 4).

The DMAP-assisted carboxylation of the OH-end-functionalized polymers was conducted in the presence of a large excess of succinic anhydride (25 equiv). Complete conversion was confirmed by ^{1}H NMR spectroscopy as well as by MALDI-TOF spectroscopy (Figures S7, S8, and S12, Supporting Information). Subsequently, the carboxylic acids were activated with an excess of carbonyldiimidazole, which was removed subsequently by precipitation of the polymer in acetone. The imidazole amide-terminated PF was further reacted with mono amino-functionalized polyethylene glycole, CH_3O-$(CH_2CH_2O)_nCH_2CH_2NH_2$ (2 × 10^3 g mol^{-1}). The formation of the desired block copolymer was confirmed by ^{1}H NMR spectroscopy (Figures S9 and S10, Supporting Information). The integrals of the H_3CO-PEG-end group and the succinylene protons indicate a 1:1 stoichiometry, underlining a complete PEGylation of the polyfluorene and successful removal of unreacted excess PEG-amine starting material. The PMI-

dx.doi.org/10.1021/ja311497e | J. Am. Chem. Soc. 2013, 135, 1148−1154

Scheme 4. Synthesis of Amphiphilic Block Copolymers Starting from PF1 (Including Gray Branch) or PF2 (Excludes Gray Branch)

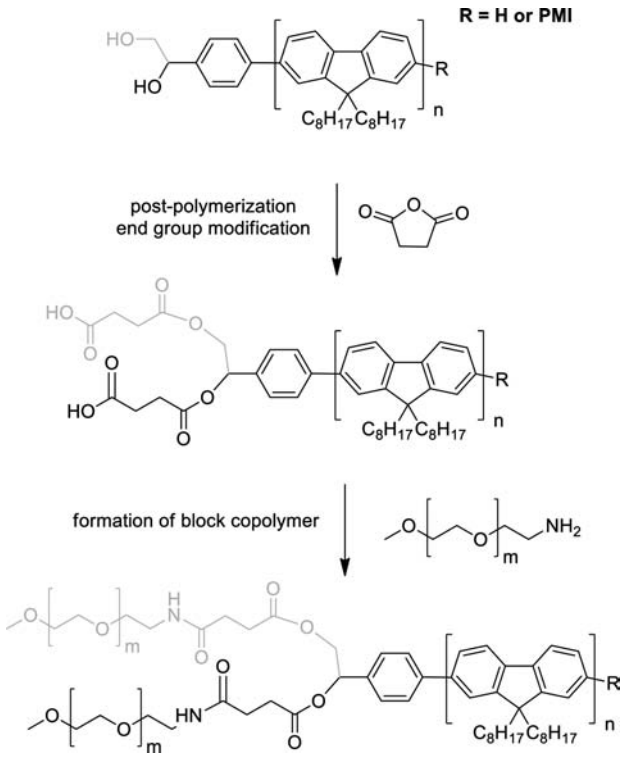

substituted PF was reacted in an identical manner to yield the amphiphilic PMI labeled block copolymer PMI-PF-PEG.

For the preparation of aqueous nanoparticle dispersions from these amphiphilic block copolymers, the nanoprecipitation technique was applied.[9a,17] A dilute solution of polymer in a water miscible solvent is quickly added to rapidly stirred water. This results in polymer nanoparticles, which are stabilized by the hydrophilic block. For the formation of polyfluorene nanoparticles, 0.05 wt % THF solutions of PF-PEG or PMI-PF-PEG were nanoprecipitated in Milli-Q water to yield aqueous dispersion with 0.003 wt % polymer content. Particles exhibited an excellent stability over time as evidenced by unaltered particle sizes measured by DLS even after weeks and months. These nanoparticles possess a spherical shape and diameters of 25−50 nm as evidenced by TEM imaging (Figure 3). A general tendency that increasing PF block lengths lead to an increase in particle diameters was indicated by DLS measurements. For example, nanoparticle preparation from a block copolymer with a 4.7×10^3 g mol^{-1} PF block and a 2.0×10^3 g mol^{-1} PEG block resulted in a number average particle diameter of 25 nm, whereas the 4-fold PF block length led to a particle diameter of 50 nm. Amphiphilic block copolymers derived from **PF1** and **PF2** distinguished by covalent attachment of two versus one PEG block, respectively, did not exhibit any significant differences in particle size at equal PF block molecular weights.

One of the most important characteristics of polyfluorenes and conjugated polymers in general are their optical properties distinguished by a bright fluorescence emission. The polyfluorene nanoparticles possess an intenese blue to green fluorescence with fluorescence quantum yields as high as Φ = 84%.[18] The emission wavelength of these dispersions can be adjusted by furnishing PF-PEG particles with a red emitting perylene monoimide (PMI) dye, to which an energy transfer

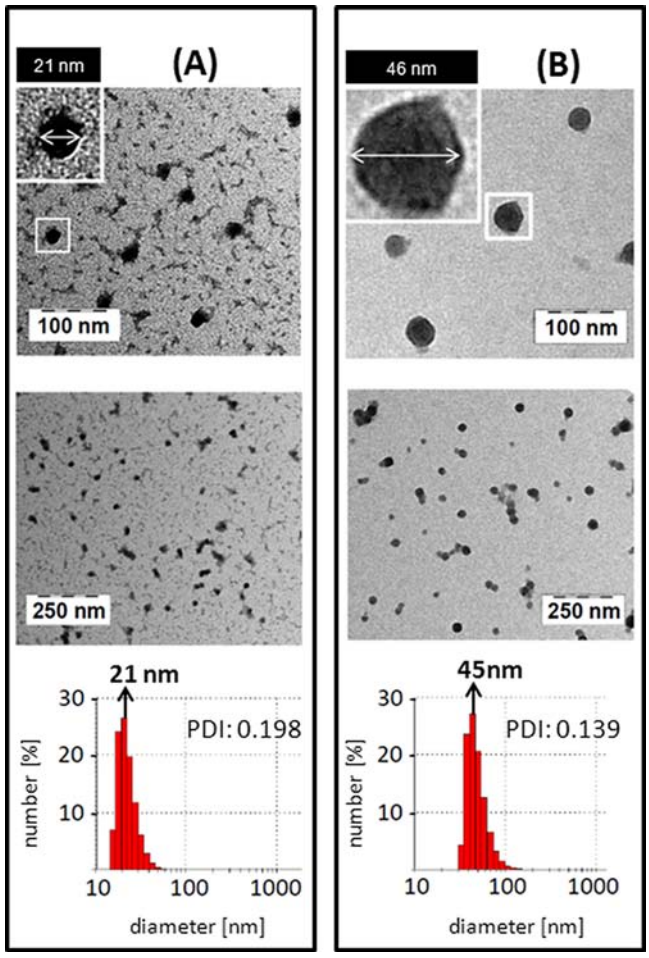

Figure 3. TEM images (top and center) and DLS measurements (bottom) of PF-PEG nanoparticles. (A) M_n(PF-block) = 4.7×10^3 g mol^{-1}. (B) M_n(PF-block) = 1.7×10^4 g mol^{-1}.

can occur.[19] As illustrated in Figure 4A, this can be performed either by blending PMI-end functionalized PF-PEG block copolymer into PF-PEG particles (system A), or by "doping" PF-PEG particles with free PMI molecules (system B). With increasing PMI content in the polymer, the emission band of the perylene imide dye at 600 nm grows in intensity along with a simultaneous decrease in the PF emission at 450 nm. This energy transfer is significantly more efficient for the covalently bound PMI system than for the PF-PEG nanoparticle dispersions with free dye molecules physically mixed with the polymer matrix (Figure 4D and E). Remarkably, at a dye content of only 5 wt % PMI relative to PF (that is, for system A a 1:1 mixture of dye-labeled and unlabeled PF block copolymer), this energy transfer from the PF matrix to the dye is virtually complete for the nanoparticles from block copolymer with covalently attached dye, while there is still notable polyfluorene emission for the physical mixture (Figure 4E). At the same time, fluorescence quantum yields are higher for the polyfluorene block copolymers with covalently bound dye end groups than with free dye (Figure 4B). With increasing dye content, both systems tend to lower quantum yields, but the decrease is substantially more pronounced for the comparative system with only physically mixed free PMI dye molecules. This effect becomes more dramatic over time, as quantum yields of PMI-PF-PEG particles remain virtually unchanged for weeks, whereas those for the system with free

dx.doi.org/10.1021/ja311497e | J. Am. Chem. Soc. 2013, 135, 1148−1154

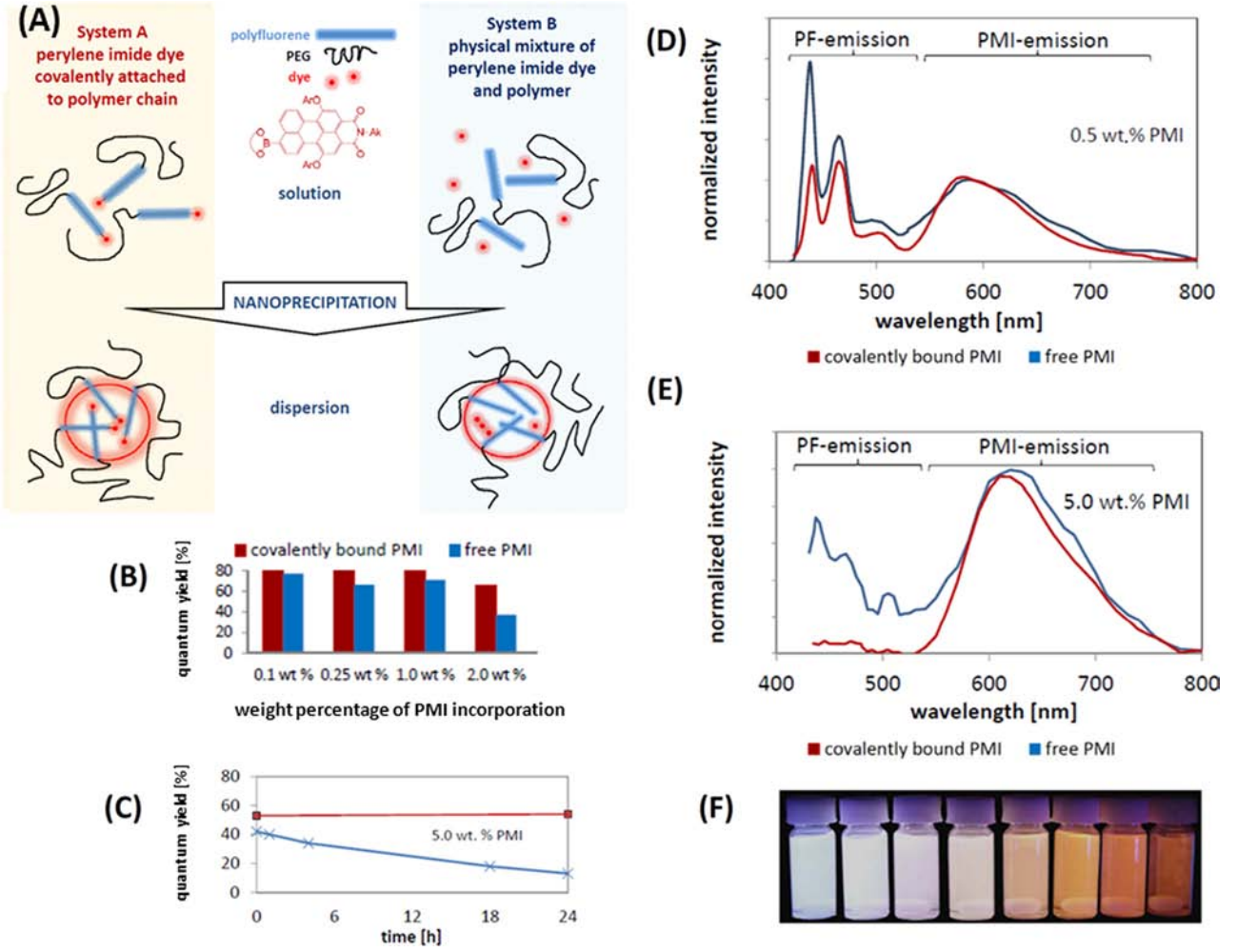

Figure 4. Emission properties of perylene monoimide (PMI)-functionalized polyfluorene-*block*-polyethylene glycol (PF-PEG) copolymer nanoparticle dispersions. (A) Scheme illustrating the two different preparation pathways for incorporation of PMI in PF-PEG nanoparticles. PMI content in system A is adjusted by addition of non-dye labeled PF-PEG copolymer. (B) Fluorescence quantum yields at various dye concentrations for polymer-bound PMI molecules (red) and physical mixtures of free PMI molecules and the polyfluorene matrix (blue). (C) Comparison of the development of fluorescence quantum yields over time of nanoparticle dispersions at 5 wt % PMI content of system A (red) versus system B (blue). (D and E) Emission spectra of (PMI-)PF-PEG nanoparticle dispersions at 0.5 and 5.0 wt % PMI concentration, respectively. Dispersions were excited at the PF absorption maximum at λ_{exc} = 388 nm. (F) Photograph of PMI-PF-PEG dispersions with increasing perylene imide content from 0.1 wt % (left) to 10 wt % (right) under UV irradiation.

dye molecules drop to values between 10% and 20% within days (Figure 4C). This behavior is attributed to an eventual aggregation of free dye molecules in the PF matrix. A certain degree of mobility within the polyfluorene matrix may lead to π-stacking of the dye molecules and subsequent nonradiative energy dissipation pathways. This clearly indicates the merits of well-defined hetero difunctional polyfluorene dye-labeled block copolymer as building blocks for nanoparticles, in which the emitter is covalently bound to the light-harvesting polymer matrix.

An emission in the deep red and near-infrared red (NIR) regime is advantageous, for example, in biological imaging due to the deeper penetrating nature by comparison to visible light of shorter wavelength. However, the energy transfer efficiency from polyfluorene to most NIR dyes is negligible, due to the lack of a spectral overlap. To this end, the heterodifunctional polyfluorenes studied here offer themselves for an energy transfer cascade. The red-emitting PMI-PF-PEG block copolymer nanoparticles and common NIR dyes exhibit a good spectral overlap of the particle emission and NIR dye absorption spectra (Figure 5A).

Nanoparticles of the PMI-functionalized block copolymers thus were "doped" with terrylene diimide (TDI), a NIR dye that emits above 660 nm. This system indeed acts as an energy transfer cascade from the polyfluorene to PMI, and from the latter to TDI, as anticipated. With increasing NIR dye content, the TDI emission band at 720 nm grows with a simultaneous decrease in the PMI emission at 600 nm (Figure 5B). As observed with physical mixtures of PMI (vide supra), increasing the "dopant" content again lowers the quantum yields. Above 2 wt % "dopant" concentration, however, the nanoparticles still show satisfactory quantum yields of 10−20%. In extension of the concept reported here, quantum yields can likely be improved by covalent binding of TDI to polyfluorene chain ends. Without PMI as "cascade intermediate", energy transfer from polyfluorene to TDI occurs to a notably smaller extent, and the polyfluorene emission is not efficiently quenched (Figure S14, Supporting Information).

dx.doi.org/10.1021/ja311497e | *J. Am. Chem. Soc.* 2013, 135, 1148−1154

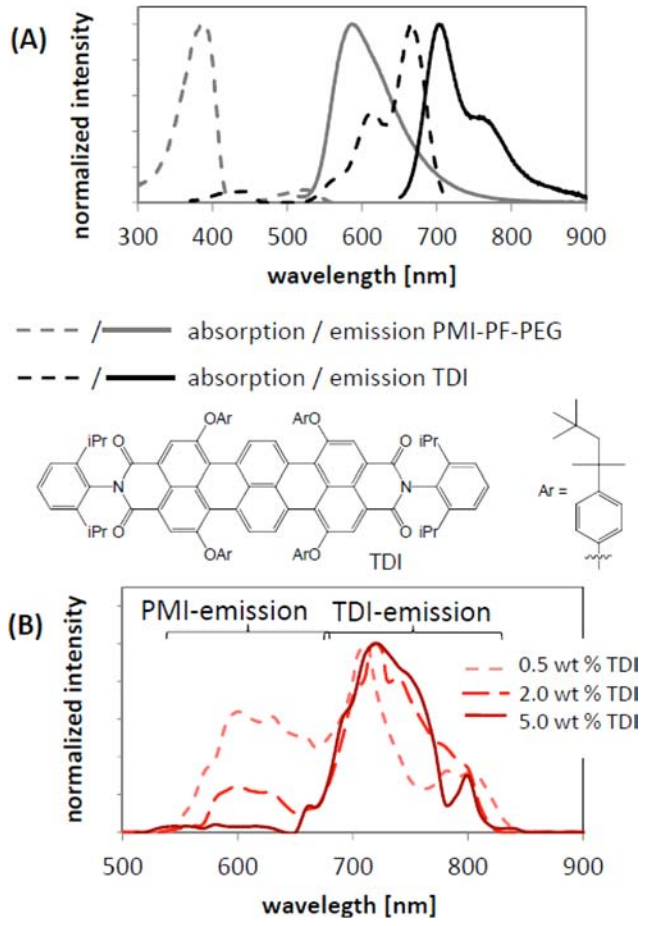

Figure 5. (A) Absorption (dashed lines) and emission (solid lines) spectra of the PMI-PF-PEG dispersions (gray) and THF-solution spectra of the terrylene diimide dye (TDI, black). (B) Emission spectra of TDI doped PMI-PF-PEG nanoparticle dispersion at various dopant concentrations. Dispersions were excited at the PF absorption maximum at λ_{exc} = 388 nm.

SUMMARY AND CONCLUSION

Novel three-coordinate palladium(II) aryl complexes with functional-group-substituted phenyl groups allow for a controlled Suzuki–Miyaura chain-growth type polymerization to yield polyfluorenes with reactive end groups. The reaction occurs with high precision, to yield polyfluorenes fully functionalized with a single end group, amenable to further reactions after deprotection. This approach strongly enhances the general utility of this elegant controlled polymerization approach to polyfluorenes, and opens routes to interesting and useful polyfluorene architectures. This is illustrated here by the synthesis of amphiphilic block copolymers via postpolymerization coupling of the functionalized reactive end groups. As the second end group, these precise heterodisubstituted polyfluorenes contain a perylene monoimide dye moiety. These well-defined block copolymers allow for the synthesis of self-stabilized very stable polyfluorene nanoparticles as small as 25 nm, without the need for any additional stabilizers. The heterodifunctional nature of these block copolymers, with a perylene dye end group, was found to be crucial for an efficient and reliable tuning of the particles' emission wavelength. By comparison, physical mixtures with the free dye featured lower quantum yields, which further decreased strongly with time, likely due to aggregation of the mobile free dye molecules. Furthermore, this concept allows for shifting the nanoparticles' emission into the deep red and near-infrared regime via an energy cascade enabled by the appropriate spectral overlap of the polyfluorene block copolymer dye end group with suitable NIR dyes, as demonstrated for terrylene diimide "doped" nanoparticles.

In summary, this enhanced synthetic approach provides precise heterodifunctional polyfluorenes and block copolymers, which can function as a future toolbox for the generation of bright luminescent nanoparticles with a well-defined surface chemistry and variable emission.

ASSOCIATED CONTENT

Supporting Information

All experimental procedures as well as ^{1}H NMR and additional MALDI-TOF spectra. This material is available free of charge via the Internet at http://pubs.acs.org.

AUTHOR INFORMATION

Corresponding Author

stefan.mecking@uni-konstanz.de

Notes

The authors declare no competing financial interest.

ACKNOWLEDGMENTS

Financial support by the DFG (Me1388/7-1) is gratefully acknowledged. We thank Lars Bolk for GPC, Marina Krumova for TEM, and Andreas Marquardt for MALDI-TOF measurements. C.S.F. thanks Alexander Letzel for participation in some of this work as a part of his undergraduate studies and M.C.B. thanks the "Fonds der Chemischen Industrie" for a scholarship.

REFERENCES

(1) Kietzke, T.; Neher, D.; Landfester, K.; Montenegro, R.; Güntner, B.; Scherf, U. *Nat. Mater.* **2003**, *2*, 408–412.

(2) Piok, T.; Gamerith, S.; Gadermaier, C.; Plank, H.; Wenzl, F.; Patil, S.; Montenegro, R.; Kietzke, T.; Neher, D.; Scherf, U.; Landfester, K.; List, E. *Adv. Mater.* **2003**, *15*, 800–804.

(3) Pecher, J.; Huber, J.; Winterhalder, M.; Zumbusch, A.; Mecking, S. *Biomacromolecules* **2010**, *11*, 2776–2780.

(4) Michalet, X.; Pinaud, F. F.; Bentolila, L. A.; Tsay, J. M.; Doose, S.; Li, J. J.; Sundaresan, G.; Wu, A. M.; Gambhir, S. S.; Weiss, S. *Science* **2005**, *307*, 538–544.

(5) Akbulut, M.; Ginart, P.; Gindy, M. E.; Theriault, C.; Chin, K. H.; Soboyejo, W.; Prud'homme, R. K. *Adv. Funct. Mater.* **2009**, *19*, 718–725.

(6) Sokolov, I.; Naik, S. *Small* **2008**, *4*, 934–939.

(7) (a) Tian, Z.; Shaller, A. D.; Li, A. D. Q. *Chem. Commun.* **2009**, 180–182. (b) Tallury, P.; Kar, S.; Bamrungsap, S.; Huang, Y.-F.; Tan, W.; Santra, S. *Chem. Commun.* **2009**, 2347–2349.

(8) (a) Yasukuni, R.; Asahi, T.; Sugiyama, T.; Masuhara, H.; Silwa, M.; Hofkens, J.; De Schryver, F. C.; Van der Auweraer, M.; Herrmann, A.; Müllen, K. *Appl. Phys. A: Mater. Sci. Process.* **2008**, *93*, 5–9. (b) Abbel, R.; Van der Weegen, R.; Meijer, E. W.; Schenning, A. P. H. J. *Chem. Commun.* **2009**, 1697–1699.

(9) (a) Wu, C.; Bull, B.; Szymanski, C.; Christensen, K.; McNeill, J. *ACS Nano* **2008**, *2*, 2415–2423. (b) Baier, M. C.; Huber, J.; Mecking, S. *J. Am. Chem. Soc.* **2009**, *131*, 14267–14273. (c) Landfester, K.; Montenegro, R.; Scherf, U.; Güntner, R.; Asawapirom, U.; Patil, S.; Neher, D.; Kietzke, T. *Adv. Mater.* **2002**, *14*, 651–655. (d) Rahim, N. A. A.; McDaniel, W.; Bardon, K.; Srinivasan, S.; Vickerman, V.; So, P. T. C.; Moon, J. H. *Adv. Mater.* **2009**, *21*, 3492–3496. (e) Howes, P.; Thorogate, R.; Green, M.; Jickells, S.; Daniel, B. *Chem. Commun.* **2009**, 2490–2492. (f) Yu, J.; Wu, C.; Sahu, S. P.; Fernando, L. P.; Szymanski, C.; McNeill, J. *J. Am. Chem. Soc.* **2009**, *131*, 18410–18414. (g) Howes,

P.; Green, M.; Levitt, J.; Suhling, K.; Hughes, M. *J. Am. Chem. Soc.* **2010**, *132*, 3989−3996. (h) Huber, J.; Jung, C.; Mecking, S. *Macromolecules* **2012**, *45*, 7799−7805.
(10) Pecher, J.; Mecking, S. *Chem. Rev.* **2010**, *110*, 6260−6279.
(11) Wu, C.; Szymanski, C.; Cain, Z.; McNeill, J. *J. Am. Chem. Soc.* **2007**, *129*, 12904−12905.
(12) (a) Kietzke, T.; Neher, D.; Kumke, M.; Montenegro, R.; Landfester, K.; Scherf, U. *Macromolecules* **2004**, *37*, 4882−4890. (b) Zhang, Z.; Qiang, L.; Liu, B.; Xiao, X.; Wei, W.; Peng, B.; Huang, W. *Mater. Lett.* **2006**, *60*, 679−684. (c) Grigalevicius, S.; Forster, M.; Ellinger, S.; Landfester, K.; Scherf, U. *Macromol. Rapid Commun.* **2006**, *27*, 200−202. (d) Wu, C.; Peng, H.; Jiang, Y.; McNeill, J. *J. Phys. Chem. B* **2006**, *110*, 14148−14154. (e) Huyal, I.; Ozel, T.; Tuncel, D.; Demir, H. *Opt. Express* **2008**, *16*, 13391−13397. (f) Wu, C.; Zheng, Y.; Szymanski, C.; McNeill, J. *J. Phys. Chem. C* **2008**, *112*, 1772−1781. (g) Wu, C.; McNeill, J. *Langmuir* **2008**, *24*, 5855−5861. (h) Wu, C.; Schneider, T.; Zeigler, M.; Yu, J.; Schiro, P.; Burnham, D.; McNeill, J.; Chiu, D. *J. Am. Chem. Soc.* **2010**, *132*, 15410−15417. (i) Ibrahimova, V.; Ekiz, S.; Gezici, Ö.; Tuncel, D. *Polym. Chem.* **2011**, *2*, 2818−2824. (j) Wu, C.; Hansen, S.; Hou, Q.; Yu, J.; Zeigler, M.; Jin, Y.; Burnham, D.; McNeill, J.; Olson, J.; Chiu, D. *Angew. Chem., Int. Ed.* **2011**, *50*, 3430−3434. (k) Gao, J.; Grey, J. *Chem. Phys. Lett.* **2012**, *522*, 86−91. (l) Liu, L.; Patra, A.; Scherf, U.; Kissel, T. *Macromol. Biosci.* **2012**, *12*, 1384−1390. (m) Negele, C.; Haase, J.; Leitenstorfer, A.; Mecking, S. *ACS Macro Lett.* **2012**, *1*, 1343−1346.
(13) Yokoyama, A.; Suzuki, H.; Kubota, Y.; Ohuchi, K.; Higashimura, H.; Yokozawa, T. *J. Am. Chem. Soc.* **2007**, *129*, 7236−7237.
(14) Yokozawa, T.; Kohno, H.; Ohta, Y.; Yokoyama, A. *Macromolecules* **2010**, *43*, 7095−7100.
(15) Elmalem, E.; Biedermann, F.; Johnson, K.; Friend, R. H.; Huck, W. T. S. *J. Am. Chem. Soc.* **2012**, *134*, 17769−17777.
(16) (a) Pschirer, N.; Kohl, C.; Nolde, F.; Qu, J.; Müllen, K. *Angew. Chem., Int. Ed.* **2006**, *45*, 1401−1404. (b) Langhals, H.; Leonhard, F. European patent EP0657436, 1995. (c) Schlichting, P.; Duchscherer, B.; Seisenberger, G.; Basché, T.; Bräuchle, C.; Müllen, K. *Chem.-Eur. J.* **1999**, *5*, 2388−2395.
(17) Szymanski, C.; Wu, C.; Hooper, J.; Salazar, M.; Perdomo, A.; Dukes, A.; McNeill, J. *J. Phys. Chem. B* **2005**, *109*, 8543−8546.
(18) At low solids contents, non-PEGylated hydrophobic polymer solution can be used to obtain stable nanoparticle dispersions. Quantum yields of such nanoprecipitated PFs (optionally blended with additional PMI dye molecules) were ca. one-half of the quantum yields reported in Figure 4, thus more resembling the bulk material. It may therefore be assumed that PF-PEG nanoparticles are more loosely aggregated than their purely hydrophobic counterparts.
(19) Ego, C.; Marsitzky, D.; Becker, S.; Zhang, J.; Grimsdale, A.; Müllen, K.; MacKenzie, J.; Silva, C.; Friend, R. *J. Am. Chem. Soc.* **2003**, *125*, 437−443.